GIF GRUPO DE INTERAÇÕES FUNDAMENTAIS

CNPq

Semihard interactions at TeV energies

Thomas Ventura Iser*
Dr. Emerson Luna**

Universidade Federal do Rio Grande do Sul
thomas.iser@ufrgs.br*
luna@if.ufrgs.br**

UFRGS 85 ANOS 1934 - 2019

60 ANOS Instituto de Física

Semihard interactions at TeV energies

T. V. Iser[1,*] and E. G. S. Luna[1,†]

[1] *Instituto de Física, Universidade Federal do Rio Grande do Sul, Caixa Postal 15051, 91501-970, Porto Alegre, RS, Brazil*

We investigate the high-energy behavior of the total cross section, $\sigma_{\rm tot}$, and the ratio of the real to imaginary parts of the scattering amplitude, ρ, in both proton-proton and antiproton-proton channels. Our analysis is based on a QCD-inspired model in which the rise of the cross sections is predominantly driven by semihard processes involving gluons. We address the tension between measurements from the ATLAS/ALFA and TOTEM Collaborations, showing that independent analyses of their datasets can provide statistically consistent descriptions of the overall data, even though they do not fully reproduce the central values of the ρ parameter at $\sqrt{s} = 13$ TeV. The slight discrepancy between these central values and the model's predicted values, obtained using an asymptotic dominant crossing-even elastic scattering amplitude, points to the potential presence of an odd component in the semihard amplitude at high energies.

PACS numbers: 12.38.Lg, 13.85.Dz, 13.85.Lg

Objective

- Utilizing a **Minijet Model** for obtaining the **total cross section** and **ratio** between the **real** and **imaginary** parts of the **forward scattering amplitude** of **pp** and **$\bar{p}p$**:
  - Working on an **Eikonal representation**.
  - Using **Derivative dispersion relations.**
  - Test the model using multiple sets of **NLO PDFs.**

- Introduction
- Formalism
- The Model
- Results and Conclusions

Introduction

Collider Events

For **proton-proton** and **antiproton-proton** colliding events with **increasing energy** it is observed an **increase in the production of jets**.

- According to **QCD**, the **rise in total cross sections** in h**adronic collisions** is driven by **jets** with **transverse energy E_T** that is **much smaller** than the square of the **total center-of-mass energy s** involved in the collision.
- Named **minijets**, these originate from the **semihard scattering** of **partons**, **hard scattering** of partons carrying a **very small fraction** of their parent hadrons momentum.

Minijet Models

Since the **dominance of jet-containing events**, minijet models assume that **semihard dynamics** play a **central role** in **hadronic collisions** at **high energies**.

- **Phenomenologically** this observed rise in total cross sections can be described within an **eikonal QCD** based framework that respects both **analyticity** and **unitarity constraints**.
- Specifically, the **energy dependence** can be derived from **QCD parton model** by using s**tandard parton-parton cross sections**, **updated** sets of **parton distribution functions (PDFs)** and **cutoffs** which **restrict** the **parton-level** interactions to the **semihard regime**.

Incongruent Results

The **experimental groups ATLAS/ALFA** and **TOTEM** present incongruent results for **forward pp observables**.

- The results obtained for **$\sqrt{s}$ = 7** and **8 TeV** are especially incompatible reaching up to **2.6 σ** for **total cross section**.
- This big a difference could imply **different possible scenarios** for the **rise** of the **total cross section**.
- It is possible that the difference in results come from the **different treatment** given to the **luminosity uncertainty**.

Formalism

Profile Function and Shadowing

$$2\mathrm{Re}\{\Gamma(b,s)\} = |\Gamma(b,s)|^2 + G_{inel}(b,s)$$

- **Impossibility** for a scattering process to receive contributions **solely** from **inelastic channels**.

$$\Gamma(b,s) = 1 - e^{-\chi(b,s)}$$

- At **high energies**, the **elastic scattering amplitude** tends to become **purely imaginary**, with the **dominant** contributions coming from **purely diffractive processes**.

Shadowing

Profile Function and Scattering Amplitude

$$\Gamma(b,s) = -i \int_0^\infty q\,\mathrm{d}q\, A(s,t) J_0(bq)$$

Fourier-Bessel

Transform

$$A(s,t) = i \int b\,\mathrm{d}b\, J_0(b\sqrt{-t})\Gamma(b,s)$$

Analytic Continuation

$$\mathcal{A}_{pp}(E, t=0) = \lim_{\epsilon \to 0} \mathcal{F}(E + i\epsilon, t=0)$$
$$\mathcal{A}_{\bar{p}p}(E, t=0) = \lim_{\epsilon \to 0} \mathcal{F}(-E - i\epsilon, t=0)$$

$$E = \frac{(s - 2m^2)}{2m}$$

Crossing Symmetry

$$\mathcal{A}^{\pm}(E, t=0) = \frac{1}{2}\left[\mathcal{A}_{\bar{p}p}(E, t=0) \pm \mathcal{A}_{pp}(E, t=0)\right]$$

$$\chi^{\bar{p}p}_{pp}(s, b) = \chi^{+}(s, b) \pm \chi^{-}(s, b)$$

Analytic Continuation

$$\mathcal{A}^{\pm}(E, t=0) = \frac{1}{2}\left[\mathcal{A}_{\bar{p}p}(E, t=0) \pm \mathcal{A}_{pp}(E, t=0)\right]$$

$$\mathcal{A}^{+}(s, 0) = i \int_0^{\infty} b\, db\, \left[1 - \cosh(\chi^{-}) \exp(-\chi^{+})\right]$$

$$\mathcal{A}^{-}(s, 0) = i \int_0^{\infty} b\, db\, \sinh(\chi^{-}) \exp(-\chi^{+})$$

$$s \gg m^2$$

Dispersion Relations

$$\chi_I^+(s,b) = -\frac{2s}{\pi}\mathcal{P}\int_0^\infty ds' \frac{\chi_R^+(s',b)}{s'^2 - s^2}$$

$$\chi_I^-(s,b) = -\frac{2s^2}{\pi}\mathcal{P}\int_0^\infty ds' \frac{\chi_R^-(s',b)}{s'(s'^2 - s^2)}$$

Derivative Dispersion Relations

$$\frac{\mathrm{Re}\{\chi^+\}(s)}{s} = \tan\left[\frac{\pi}{2}\frac{d}{d\ln s}\right]\frac{\mathrm{Im}\{\chi^+\}(s)}{s}$$

$$\frac{\mathrm{Re}\{\chi^-\}(s)}{s} = -\cot\left[\frac{\pi}{2}\frac{d}{d\ln s}\right]\frac{\mathrm{Im}\{\chi^-\}(s)}{s}$$

$$\mathrm{Im}\{\chi_{\mathrm{SH}}\}(s,b) = -\left[\frac{\pi}{2}\frac{d}{d\ln s} + \frac{1}{3}\left(\frac{\pi}{2}\frac{d}{d\ln s}\right)^3 + \frac{2}{5}\left(\frac{\pi}{2}\frac{d}{d\ln s}\right)^5 + \cdots\right]\mathrm{Re}\{\chi_{\mathrm{SH}}\}(s,b)$$

The Model

Eikonal Function

$$\chi^{\bar{p}p}_{pp}(s,b) = \chi^{+}(s,b) \pm \chi^{-}(s,b)$$

$$\chi(s,b) = \mathrm{Re}\chi(s,b) + \mathrm{Im}\chi(s,b) \equiv \chi_R(s,b) + i\chi_I(s,b)$$

$$\chi(s,b) = \chi_{soft}(s,b) + \chi_{SH}(s,b)$$

Semihard Contribution

$$\mathrm{Re}\left\{\chi_{SH}(s,b)\right\} = \frac{1}{2} W_{SH}(b)\sigma_{QCD}(s)$$

$$W_{SH}(b) = \int \mathrm{d}^2b'\, \rho_A\left(|\mathbf{b}-\mathbf{b}'|\right)\rho_B(b')$$

C. A. S. Bahia, M. Broilo, and E. G. S. Luna, Phys. Rev. D 92, 074039 (2015).

Soft Contribution

Even

$$\chi^{+}_{soft}(s,b) = \frac{1}{2} W^{+}_{soft}(b;\mu^{+}_{soft}) \left[A' + iB' + C' \frac{e^{i\pi\gamma/2}}{(s/s_0)^{\gamma}} \right]$$

Odd

$$\chi^{-}_{soft}(s,b) = \frac{1}{2} W^{-}_{soft}(b;\mu^{-}_{soft})\, D' \frac{e^{-i\pi/4}}{\sqrt{s/s_0}}$$

Form Factor and Overlap Density

$$W(b) = \int \mathrm{d}^2 b' \, \rho_A(|\mathbf{b} - \mathbf{b}'|)\rho(b')$$
$$= \frac{1}{2\pi} \int_0^\infty \mathrm{d}k_\perp \, k_\perp J_0(k_\perp b) G_A(k_\perp) G_B(k_\perp)$$
$$G_A(k_\perp) = G_B(k_\perp) \equiv G_{dip}(k_\perp; \mu) = \left(\frac{\mu^2}{k_\perp^2 + \mu^2} \right)^2$$

$$W_{SH}(b; \nu_{SH}) = \frac{\nu_{SH}^2}{96\pi} (\nu_{SH} b)^3 K_3(\nu_{SH} b)$$

$$\rho(b) = \frac{1}{(2\pi)^2} \int \mathrm{d}k_\perp G(k_\perp) e^{i\mathbf{k}_\perp \cdot \mathbf{b}}$$

QCD Cross Section

$$\sigma_{QCD}(s) = \sum_{i,j,k,l} \int_{p_{Tmin}}^{s/4} \mathrm{d}p_T^2 \int_{4p_T^2/s}^{1} \mathrm{d}x_1 \int_{4p_T^2/x_1 s}^{1} \mathrm{d}x_2$$
$$\times \left[f_{i/A}(x_1, Q^2) f_{j/B}(x_2, Q^2) + f_{j/A}(x_1, Q^2) f_{i/B}(x_2, Q^2) \right]$$
$$\times \left[\frac{\mathrm{d}\hat{\sigma}_{ij\to kl}}{\mathrm{d}p_T^2}(\hat{t}, \hat{u}) + \frac{\mathrm{d}\hat{\sigma}_{ij\to kl}}{\mathrm{d}p_T^2}(\hat{u}, \hat{t}) \right] (1 - \delta_{ij}/2)(1 - \delta_{kl}/2)$$

$$\frac{\mathrm{d}\hat{\sigma}}{\mathrm{d}p_T^2} = \frac{\mathrm{d}\hat{\sigma}}{\mathrm{d}(-\hat{t})} \frac{\mathrm{d}(-\hat{t})}{\mathrm{d}p_T^2} = \frac{\mathrm{d}\hat{\sigma}}{\mathrm{d}(-\hat{t})} \frac{1}{\sqrt{1 - 4\frac{p_T^2}{\hat{s}}}} = \frac{\mathrm{d}\hat{\sigma}}{\mathrm{d}|\hat{t}|} \frac{1}{\sqrt{1 - 4\frac{p_T^2}{\hat{s}}}}$$

Parton-level processes

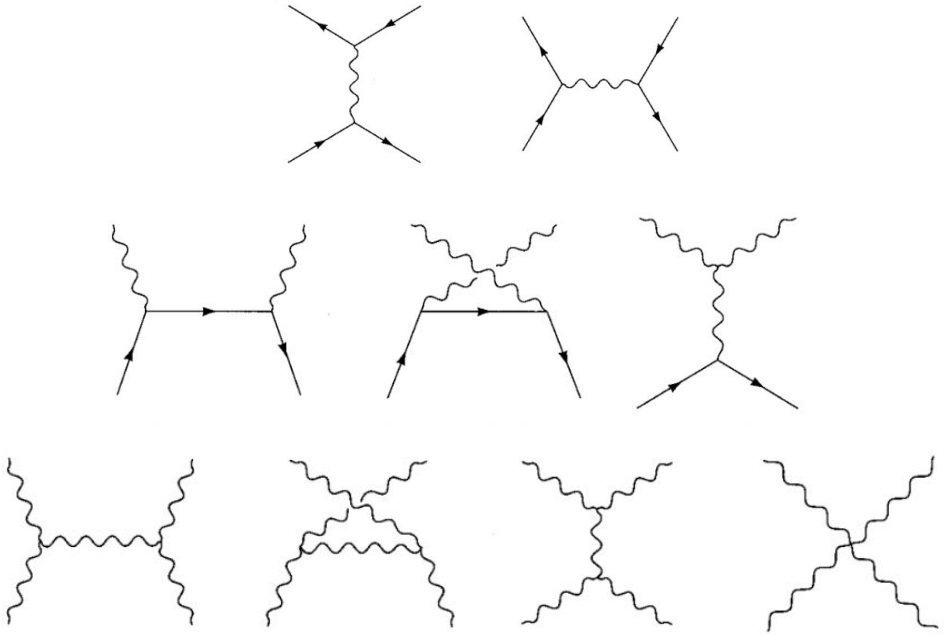

Subprocesso	Seção de choque partônicas
$qq' \to qq'$	$\frac{4}{9}\frac{\hat{s}^2+\hat{u}^2}{\hat{t}^2}$
$qq \to qq$	$\frac{4}{9}\left[\frac{\hat{s}^2+\hat{u}^2}{\hat{t}^2}+\frac{\hat{s}^2+\hat{t}^2}{\hat{u}^2}\right]-\frac{8}{27}\frac{\hat{s}^2}{\hat{t}\hat{u}}$
$q\bar{q} \to q'\bar{q}'$	$\frac{4}{9}\frac{\hat{t}^2+\hat{u}^2}{\hat{s}^2}$
$q\bar{q} \to q\bar{q}$	$\frac{4}{9}\left[\frac{\hat{s}^2+\hat{u}^2}{\hat{t}^2}+\frac{\hat{u}^2+\hat{t}^2}{\hat{s}^2}\right]-\frac{8}{27}\frac{\hat{u}^2}{\hat{s}\hat{t}}$
$gq \to gq$	$-\frac{4}{9}\left[\frac{\hat{s}}{\hat{u}}+\frac{\hat{u}}{\hat{s}}\right]+\frac{\hat{s}^2+\hat{u}^2}{\hat{t}^2}$
$q\bar{q} \to gg$	$\frac{32}{27}\left[\frac{\hat{t}}{\hat{u}}+\frac{\hat{u}}{\hat{t}}\right]-\frac{8}{3}\frac{\hat{t}^2+\hat{u}^2}{\hat{s}^2}$
$gg \to q\bar{q}$	$\frac{1}{6}\left[\frac{\hat{t}}{\hat{u}}+\frac{\hat{u}}{\hat{t}}\right]-\frac{3}{8}\frac{\hat{t}^2+\hat{u}^2}{\hat{s}^2}$
$gg \to gg$	$\frac{9}{2}\left[3-\frac{\hat{t}\hat{u}}{\hat{s}^2}-\frac{\hat{s}\hat{u}}{\hat{t}^2}-\frac{\hat{s}\hat{t}}{\hat{u}^2}\right]$

Parton Distribution Functions (PDF)

- Comparison between the **gluon PDF** behaviors of the **three** selected sets at **four different energy scales**.
- It can be observed that the **behavior** at **high energy scales** is practically the **same**, as expected.
- At low energies, the behaviors start to **diverge**, and near the **limiting scale** suggested by Gribov, they become completely different at **small x**.
- Since these **energy scales** and **momentum fractions** are the most **significant** for the model, the **need for different sets** becomes evident.

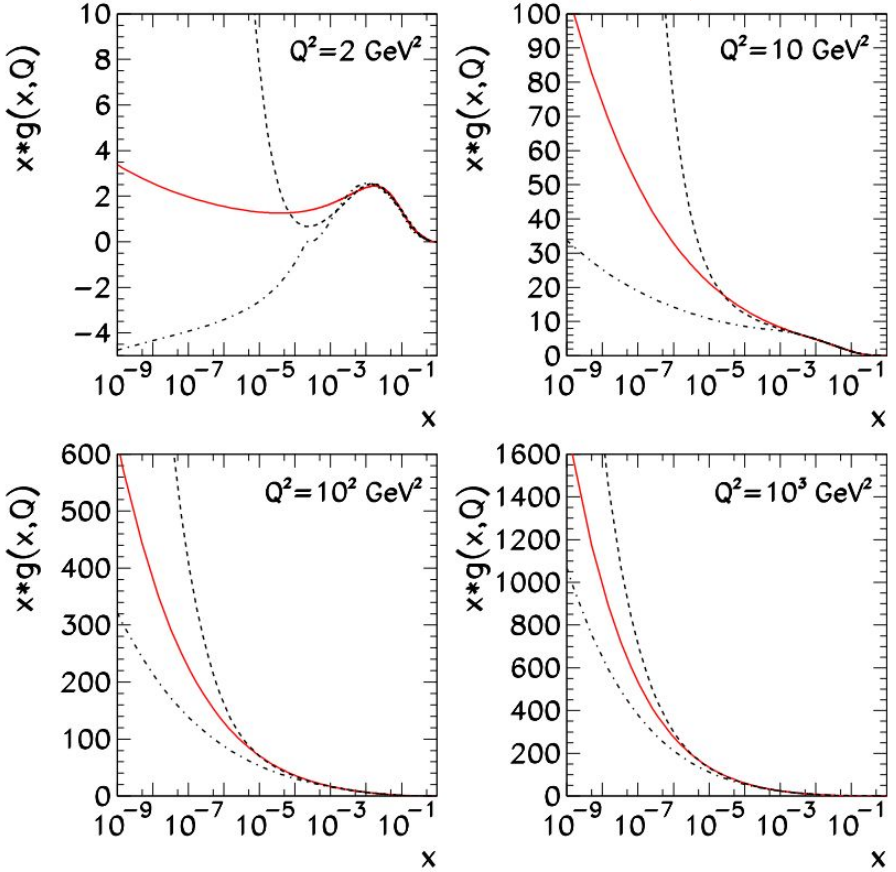

Eikonal Representation - Observables

$$\sigma_{el}(s) = 2\pi \int_0^\infty b\,\mathrm{d}b\,|\Gamma(b,s)|^2$$
$$= 2\pi \int_0^\infty b\,\mathrm{d}b\,|1 - e^{-\chi_I(b,s)+i\chi_R(b,s)}|^2$$

$$\sigma_{inel}(s) = 2\pi \int_0^\infty b\,\mathrm{d}b\,G_{inel}(b,s)$$
$$= 2\pi \int_0^\infty b\,\mathrm{d}b\,\left[1 - e^{-2\chi_I(b,s)}\right]$$

$$2\mathrm{Re}\{\Gamma(b,s)\} = |\Gamma(b,s)|^2 + G_{inel}(b,s)$$

$$\sigma_{tot}(s) = 4\pi \int_0^\infty b\,\mathrm{d}b\,\mathrm{Re}\{\Gamma(b,s)\}$$
$$= 4\pi \int_0^\infty b\,\mathrm{d}b\,\left[1 - e^{-\chi_I(b,s)}\cos\chi_R(b,s)\right]$$

$$\rho(s) = \frac{\mathrm{Re}\{i\int b\,\mathrm{d}b[1 - e^{i\chi(b,s)}]\}}{\mathrm{Im}\{i\int b\,\mathrm{d}b[1 - e^{i\chi(b,s)}]\}}$$

$$\Gamma(b,s) \equiv 1 - e^{i\chi(b,s)}$$

Results and Conclusions

Analysis

- The global fits were obtained through a χ^2 minimization procedure, with confidence regions defined by the interval χ^2-χ^2_{min} corresponding to the 90% confidence level.

- $\sigma_{tot}^{pp,p\bar{p}}(10\,\text{GeV} < \sqrt{s} < 1.8\,\text{TeV};\ \mathbf{PDG}) + \rho^{pp,p\bar{p}}(10\,\text{GeV} < \sqrt{s} < 1.8\,\text{TeV};\ \mathbf{PDG}) + \sigma_{tot}^{pp}(7, 8, 13\,\text{TeV};\ \mathbf{ATLAS}) + \rho^{pp}(7, 8, 13\,\text{TeV};\ \mathbf{ATLAS})$

- $\sigma_{tot}^{pp,p\bar{p}}(10\,\text{GeV} < \sqrt{s} < 1.8\,\text{TeV};\ \mathbf{PDG}) + \rho^{pp,p\bar{p}}(10\,\text{GeV} < \sqrt{s} < 1.8\,\text{TeV};\ \mathbf{PDG}) + \sigma_{tot}^{pp}(2.76, 7, 8, 13\,\text{TeV};\ \mathbf{TOTEM}) + \rho^{pp}(2.76, 7, 8, 13\,\text{TeV};\ \mathbf{TOTEM})$

Fit Parameters

$$\sigma_{QCD}(s) = \mathcal{N} \sum_{i,j,k,l} \int_{p_{Tmin}}^{s/4} \mathrm{d}p_T^2 \int_{4p_T^2/s}^{1} \mathrm{d}x_1 \int_{4p_T^2/x_1 s}^{1} \mathrm{d}x_2$$
$$\times \left[f_{i/A}(x_1, Q^2) f_{j/B}(x_2, Q^2) + f_{j/A}(x_1, Q^2) f_{i/B}(x_2, Q^2) \right]$$
$$\times \left[\frac{\mathrm{d}\hat{\sigma}_{ij\to kl}}{\mathrm{d}p_T^2}(\hat{t}, \hat{u}) + \frac{\mathrm{d}\hat{\sigma}_{ij\to kl}}{\mathrm{d}p_T^2}(\hat{u}, \hat{t}) \right] (1 - \delta_{ij}/2)(1 - \delta_{kl}/2)$$

$$W_{SH}(b; \nu_{SH}) = \frac{\nu_{SH}^2}{96\pi} (\nu_{SH} b)^3 K_3(\nu_{SH} b)$$

Fit Parameters

Even

$$\chi^{+}_{soft}(s,b) = \frac{1}{2} W^{+}_{soft}(b;\mu^{+}_{soft}) \left[A' + iB' + C' \frac{e^{i\pi\gamma/2}}{(s/s_0)^{\gamma}} \right]$$

Odd

$$\chi^{-}_{soft}(s,b) = \frac{1}{2} W^{-}_{soft}(b;\mu^{-}_{soft})\, D' \frac{e^{-i\pi/4}}{\sqrt{s/s_0}}$$

ALFA/ATLAS

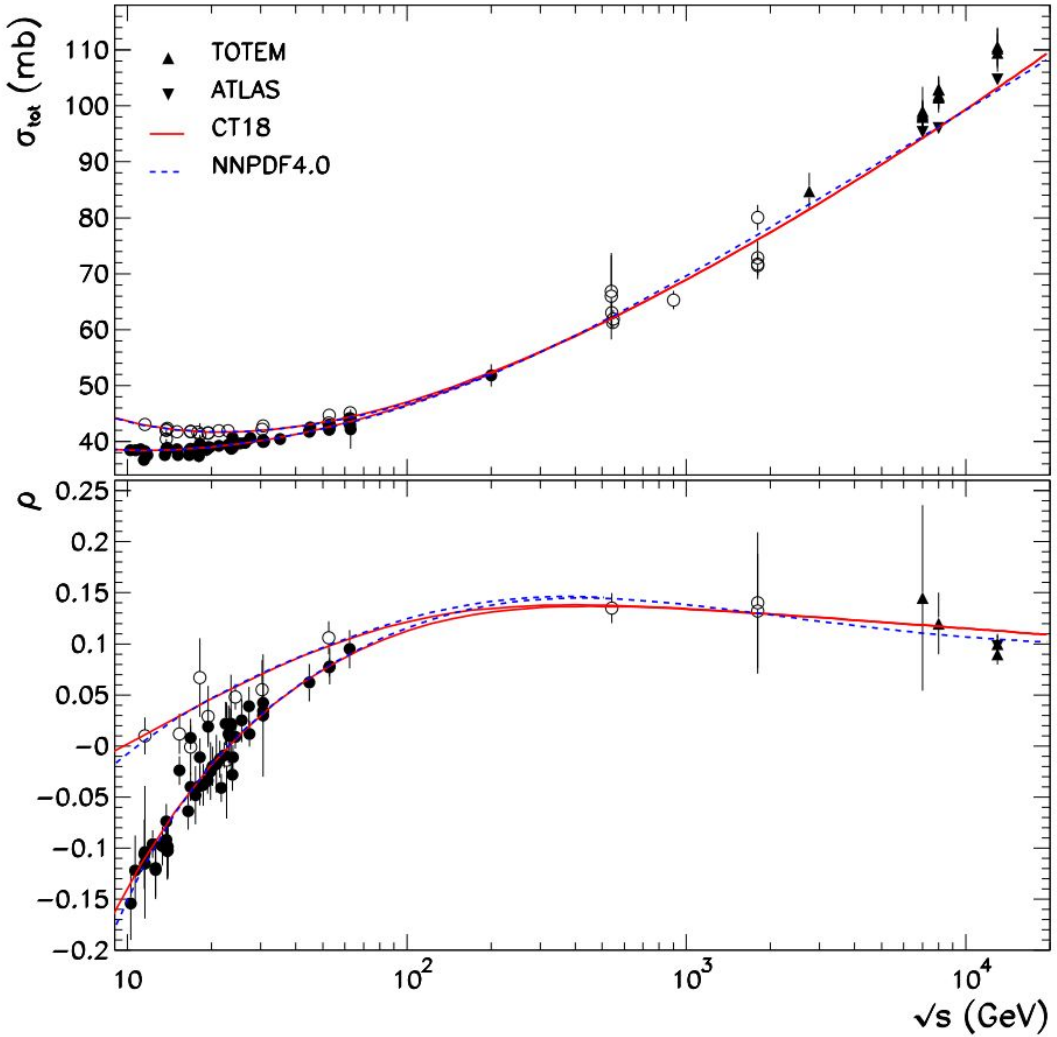

	CT18	NNPDF4.0
	$p_{Tmin} = 1.1\,\text{GeV}$	$p_{Tmin} = 1.3\,\text{GeV}$
$\mathcal{N}$	1.83 ± 0.46	1.53 ± 0.57
ν_{SH} [GeV]	1.418 ± 0.084	1.12 ± 0.12
A [GeV^{-2}]	$(2.1 \pm 2.0) \times 10^3$	$(3.9 \pm 4.9) \times 10^2$
B [GeV^{-2}]	-76 ± 148	-14 ± 26
C [GeV^{-2}]	$(31 \pm 36) \times 10^3$	$(4.5 \pm 7.6) \times 10^3$
μ^+_{soft} [GeV]	2.55 ± 0.39	1.78 ± 0.67
D [GeV^{-2}]	150 ± 11	147 ± 12
ν	158	158
χ^2/ν	1.10	1.07

TOTEM

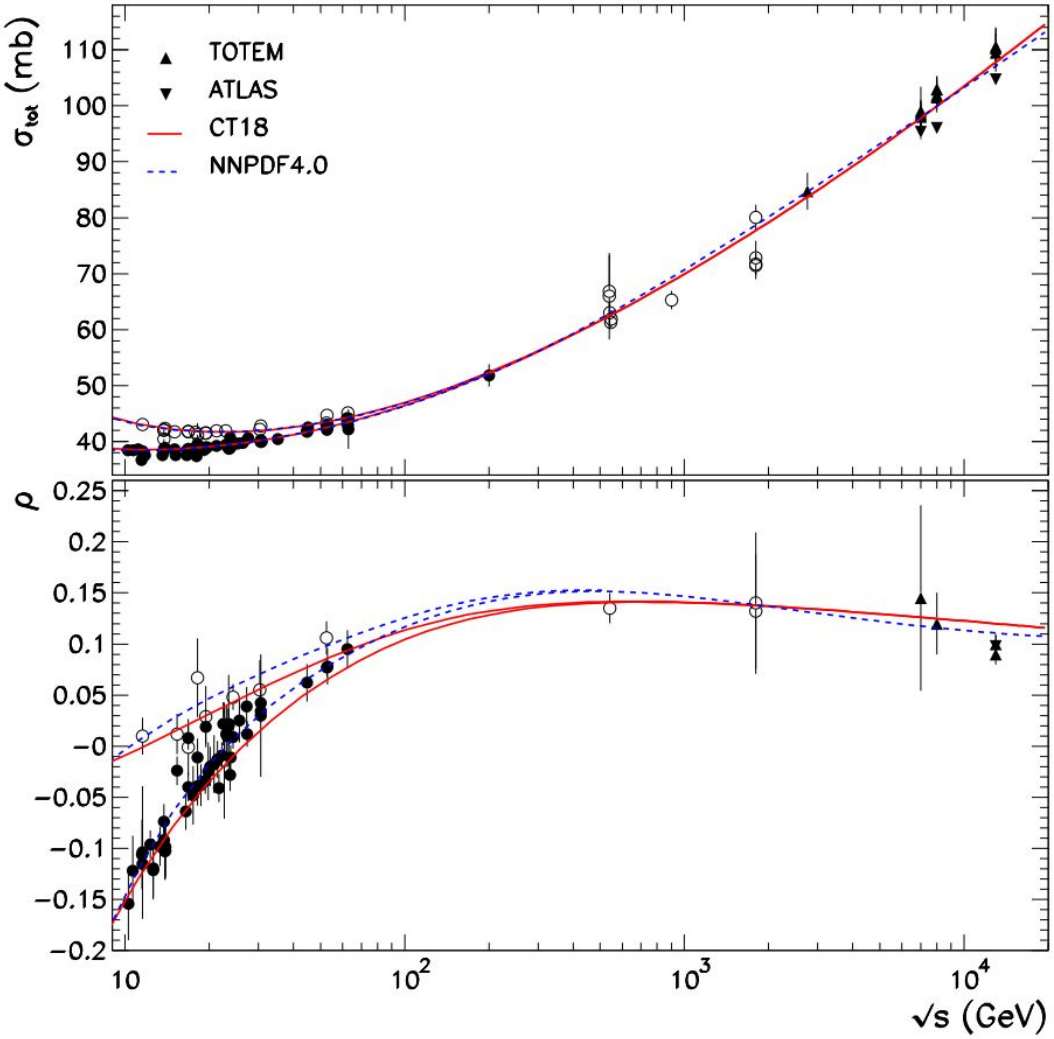

	CT18	NNPDF4.0
	$p_{Tmin} = 1.1\,\text{GeV}$	$p_{Tmin} = 1.3\,\text{GeV}$
$\mathcal{N}$	1.49 ± 0.50	1.42 ± 0.49
ν_{SH} [GeV]	1.32 ± 0.12	1.13 ± 0.11
A [GeV^{-2}]	$(2.38 \pm 0.24) \times 10^3$	$(6.3 \pm 12) \times 10^2$
B [GeV^{-2}]	-79 ± 131	-23 ± 60
C [GeV^{-2}]	$(34 \pm 11) \times 10^3$	$(8.2 \pm 20) \times 10^3$
μ^+_{soft} [GeV]	2.584 ± 0.049	2.02 ± 0.91
D [GeV^{-2}]	149 ± 11	148 ± 12
ν	168	168
χ^2/ν	1.18	1.11

Conclusions

- The model succeeds in reproducing most of the experimental range of data, notably:
  - The **ALFA/ATLAS** measurements of total cross section are well described by both **CT18** and **NNPDF4.0**. Whereas for ρ data at $\sqrt{s} = 13$ TeV only **NNPDF4.0** manages to reach its uncertainty band.
  - The **TOTEM** measurements for total cross section are also well described. As for ρ, both sets seem to fail at describing the its central value at 13 TeV, although **NNPDF4.0** reaches close.

ALFA/ATLAS

$$\sigma_{\text{tot}}^{\text{NNPDF4.0}} = 102.7 \text{ mb} \qquad \rho^{\text{NNPDF4.0}} = 0.105$$

$$\sigma_{\text{tot}}^{\text{CT18}} = 103.2 \text{ mb} \qquad \rho^{\text{CT18}} = 0.113$$

Conclusions

- The model succeeds in reproducing most of the experimental range of data, notably:
  - The **ALFA/ATLAS** measurements of total cross section are well described by both **CT18** and **NNPDF4.0**. Whereas for ρ data at $\sqrt{s}$ = 13 TeV only **NNPDF4.0** manages to reach its uncertainty band.
  - The **TOTEM** measurements for total cross section are also well described. As for ρ, both sets seem to fail at describing the its central value at 13 TeV, although **NNPDF4.0** reaches close.

TOTEM

$$\sigma_{\text{tot}}^{\text{NNPDF4.0}} = 107.1 \text{ mb} \qquad \rho^{\text{NNPDF4.0}} = 0.111$$

$$\sigma_{\text{tot}}^{\text{CT18}} = 107.8 \text{ mb} \qquad \rho^{\text{CT18}} = 0.120$$

Perspectives for the Minijet Model

- To test the inclusion of an **odd component** for the **semihard region** (**Odderon**).

- For future analyses, test **different types of form factors**, in addition to the **dipole** one.

- Extend the application of the model to describe the differential cross section at $\sqrt{s}$ **= 7 , 8** e **13 TeV**.

Thank You!!!